THE AMERICAN SOCIETY OF MECHANICAL ENGINEERS
345 E. 47 St., New York, N.Y. 10017

90-GT-140

Design and Testing of a Controlled Diffusion Airfoil Cascade for Industrial Axial Flow Compressor Application

W. STEINERT, B. EISENBERG*, H. STARKEN

Institut für Antriebstechnik
DLR, Linder Höhe, 5000 Köln 90, W.-Germany

*MAN Gutehoffnungshütte AG, Oberhausen
Bahnhofstr. 66, 4200 Oberhausen, W.-Germany

ABSTRACT

Similarly as in jet engine development, modern design methods are used today to improve the performance of industrial compressors. In order to verify the loading limits, a cascade profile representative for the first rotor hub section of an industrial compressor has been designed by optimizing the suction surface velocity distribution using a direct boundary layer calculation method. The blade shape was computed with an inverse full potential code and the resulting cascade was tested in a cascade windtunnel. The experimental results confirmed the design intent and resulted in a low loss coefficient of 1.8% at design condition and an incidence range of nearly 12° (4% loss level) at an inlet Mach number of 0.62.

NOMENCLATURE

c	chord length
H_{12}	boundary layer shape factor
M	Mach number
p	static pressure
p_t	total pressure
t/c	pitch to chord ratio
x	coordinate in chordwise direction
β	flow angle with reference to circumferential direction
β_s	stagger angle with reference to circumferential direction
η	coordinate in circumferencial direction
ω	total pressure loss coefficient $= (p_{t1} - p_{t2})/(p_{t1} - p_1)$
Ω	axial-velocity-density-ratio (AVDR)

SUBSCRIPTS

1	inlet plane
2	outlet plane

I. INTRODUCTION

Modern axial-flow compressors for industrial applications are characterized by the fact that they are always adapted to the specific requirements of the downstream process. While gas turbine compressors as a rule are operated along a performance curve which follows the pattern of a throttle curve in the performance map, industrial compressors generally must permit large mass flow variations. Therefore, it is often found that industrial compressors have to operate at design points with variations between 65% and 110% of the design mass flow, at constant pressure ratio. At the same time, a compromise must be found between the highest possible efficiency and an economic pressure ratio per stage.

The development of industrial axial-flow compressors from MAN GHH /1/ therefore centers around the following main aspects:

- Large variations in pressure ratio and flow volume for adaption to the process conditions.
- High efficiency for reducing energy costs.
- Minimum size and maximized operational reliability.

To satisfy these requirements, the various blade rows of the compressor stages must be so designed as to provide the largest possible working range between choking and separation at highest possible inlet Mach number. While the low loss range decreases with rising Mach number, a lower Mach number means larger compressor units. Therefore, an acceptable compromise has to be found between size and operating range. This leads to blading designs in a Mach number range where the influence of incidence on profile losses is comparatively low.

Axial-flow compressors of this type therefore are still using profile configurations with a subsonic inlet flow over the full blade length, because any transonic inlet

*Presented at the Gas Turbine and Aeroengine Congress and Exposition—June 11-14, 1990—Brussels, Belgium
This paper has been accepted for publication in the Transactions of the ASME
Discussion of it will be accepted at ASME Headquarters until September 30, 1990

flow would cause additional losses in efficiency by shock waves and would narrow the working range.

Although a transonic design would reduce the unit size it would still mean a lower efficiency which cannot be tolerated in the present energy situation.

On account of these conditions and in contrast to the design of gas turbine compressors, the stage pressure ratio to be selected is still comparatively low. Further, low tip speeds are limiting the max. volume that can pass through the compressor inlet. To achieve the greatest possible volumetric throughflow, a fixed size of the casing has to be chosen for reasons of cost. Therefore, industrial axial flow compressors are nowadays being built with a small hub/tip ratio around 0.45.

This, however, limits the max. number of blades that can be arranged on the rotor hub. As a result, the pitch /chord ratios in the outer sections are relatively high so that an optimal flow through the blade rows is very difficult to achieve. For this reason the outer sections are designed with comparatively small deflections. If the stage is additionally designed for constant energy transfer over the blade length, the low tip speed and long blades will produce high aerodynamic blade loads on the hub.

Since industrial axial-flow compressors must be able to cope with a wide working range every effort is made to locate operating points very near to the surge line. Special controls have been developed for this, which allow to run the compressor along an operating line parallel to the surge line with a margin of approx. 8-10%. The blade strength must be sufficient to provide adequate safety against an occasional crossing of the surge line. On account of the three aspects referred to above, i.e. large pitch/chord ratio, large profile thickness for reasons of strength, and high deflection, the profiles of the hub sections in industrial axial-flow compressors are subjected to the highest loads with respect to the diffusion factor.

As part of ongoing optimization efforts of axial-flow compressors, a front stage has been developed with the aid of advanced design methods. Requirements to be satisfied by the blading were as follows:

- Higher stage pressure ratio in the front stage.
- Improved off-design performance.
- Higher efficiency.

To meet these requirements, the blade sections were to be designed by methods which permit a controlled diffusion along the blade surfaces. These methods allow an optimization of suction and pressure side velocities in such a way that a boundary layer separation is avoided.

II. CASCADE DESIGN

Transferred to the cascade design, the above requirements for the blading led to the following aspects:

- High loading.
- Large incidence range.
- Separation-free profile boundary layers.

To meet these demands, modern design methods have to be used for the profile development to permit the velocity distribution inside the blade passage to be prescribed.

Besides the mode of solving the flow field equations (potential theory, Navier-Stokes) these methods can be subdivided into direct and inverse calculation methods. In the direct approach, the flow field is fully described by the specified cascade geometry and the flow conditions upstream and downstream of the cascade.

The inverse design method is based on the velocity distribution on the profile surfaces. These given data, the required pitch/chord ratio, and the inlet/exit flow conditions permit the associated flow channel to be defined. (Fig. 1) The inverse design method requires multiple variations of the velocity distribution until an acceptable profile geometry is obtained.

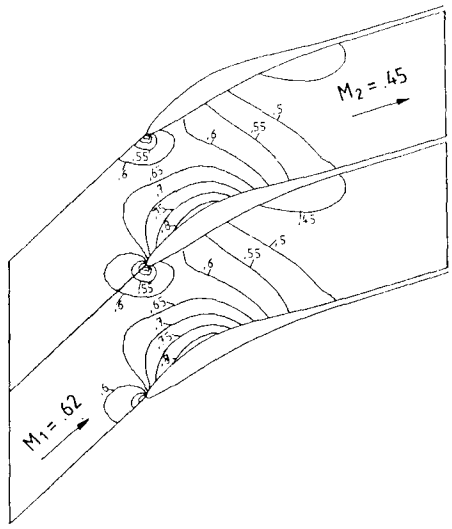

Fig.1: Calculated iso Mach lines of MAN GHH 1-S1 cascade

The answer to the question which of the two methods - direct approach by specifying the geometry with subsequent variation, or inverse approach based on a given velocity distribution - would be more suitable depends on the respective application. Where a completely new cascade design is to be developed, the inverse method is well suited if no experience is available with the cascade configuration. Unlike in the direct design practice, this permits a velocity distribution to be used in all iterations which offers optimum properties as far as its boundary layer behaviour is concerned. If, however, the profile geometry must be modified for reasons of strength, the direct method is the superior one. A typical example would be the leading edge radius which is generally prescribed by a certain size. The direct methods are also required for determining the off-design performance.

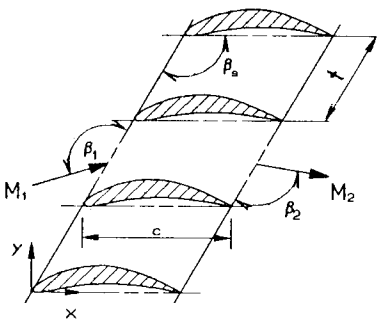

Fig.2: Definition of cascade inlet and exit flow conditions

The design project under consideration used a combination of both methods. Within a research project of "Forschungsvereinigung Verbrennungskraftmaschinen e.V." (FVV) /2-5/, an inverse and a direct calculation method for high inlet flow Mach numbers in the subsonic range were provided.

The inverse method was developed by E. Schmidt at the Stuttgart University /6//7/. It is used for calculating the steady compressible potential flow of a channel of unknown configuration. The velocity field is determined by solving the potential equation with finite differences, making full allowance for the change in type of differential equation (elliptical - hyperbolic). This approach permits the design of profiles with high subsonic inlet flow Mach numbers where local supersonic areas are formed on the profile surfaces. By prescribing an appropriate velocity distribution compression shocks can be reduced in their effect or even be fully avoided. Allowance for the variation of the axial-velocity-density-ratio is made by the introduction of a variable thickness stream layer. A distinction is made in this regard between the blockage effect of the side walls and the downstream wake region. The final metal contour is determined by subtracting the displacement thickness from the channel contour determined by the potential method. For this purpose, the integral boundary layer method of McNally /8/ is applied. The same method is used to optimize the prescribed velocity distribution required as input into the inverse method. The design under consideration was performed on a cylindrical stream surface. Meanwhile the method has been extended to also include axisymmetric stream surfaces with variable radii for both rotors and stators /9/.

The direct calculation program is based on a flux-finite-element method originally developed in 1978 by Lucchi and Schmidt /10/. This method was adapted to industrial use by "Deutsche Forschungsanstalt für Luft- und Raumfahrt e.V." (DLR) /2-5//11/. It predicts the cascade flow using potential flow theory together with the artificial density concept in supersonic flow areas. It was extended by adding the above mentioned boundary layer and a mixing calculation in an iterative mode. The effect of the boundary layer on the flow field is determined by adding the calculated displacement thicknesses to the metal profile. The present version allows local supersonic areas up to max. Mach numbers around M=1.3 as well as weak compression shocks resulting from this. The AVDR-influence is included in the calculation. The exit flow angle is determined iteratively by varying β_2 until suction and pressure surface velocity distribution meet at the trailing edge. A calculated result of the design point of this cascade with the iso Mach lines is shown in Fig. 1.

Design calculations of the 1st stage of the related test compressor have shown that the hub section was subject to the highest aerodynamic loading. The requirements for this section were as follows:

M1 = .62 M2 = .45 Betas = 120.0°
Beta1 = 137° Beta2 = 110.6°
t/c = .68 Omega = 1.1

The definitions of the above data are presented in Fig. 2.

Preliminary strength assessments of the required maximum profile thickness resulted in a value of 11% of the chord length. The initial velocity distribution was selected in such a way that the boundary layer was kept laminar as long as possible in order to reduce the minimum loss level. Behind the transition point at about 40% of chord a decreasing velocity gradient ensured a separation free turbulent diffusion up to the trailing edge. Having adjusted the velocity distribution to the required circulation and profile thickness, the Mach number distribution of Fig. 3 was obtained.

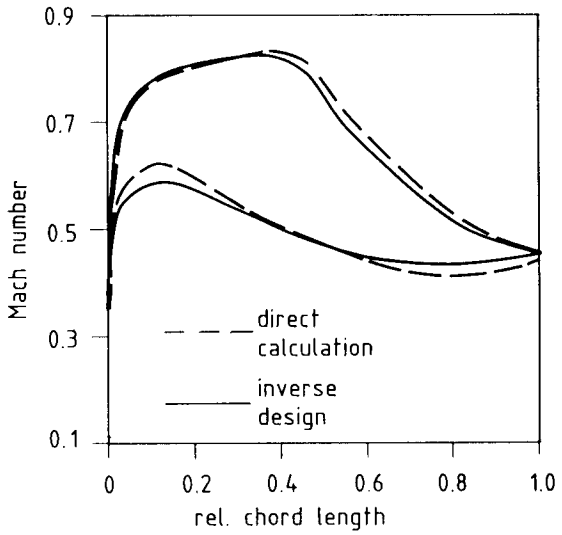

Fig.3: Mach number distribution of design and direct calculation

A precise determination of the profile contour may be problematic in certain cases, due to the fact that the velocities of the profile surfaces are specified in advance and that the profile is to be determined from the geometric difference between two calcu-

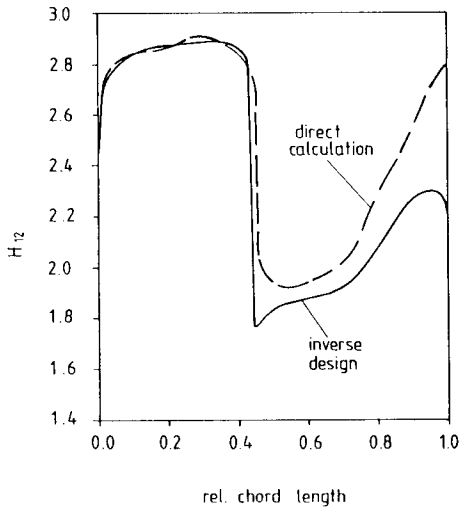

Fig.4: Shape factor development on suction side

lated periodic stream lines. The pronounced velocity gradients at the profile leading edge require a good adaption of the flow field in this area. Therefore in a recent program version the leading edge region is calculated by multiple grid refinement. Due to limited calculation time and storage capacity, the present design was performed using a simplified grid at the leading edge. The final geometry of the front section was then determined with the aid of the direct calculation program providing a leading edge radius for manufacturing.

In the design process the optimization of the loading was performed by increasing the suction surface diffusion until the boundary layer calculation approached separation, which was checked by the shape factor H_{12}. Therefore the loading limits were not determined by conventional parameters (diffusion factor, de Haller number) rather than by the boundary layer behaviour. Regarding the shape factor development it is important to notice that the boundary layer calculation using the inverse design velocity distribution was free from separation with a criterion selected as $H_{12}>2.5$. The direct-calculation, however, indicated a rise in the shape factor near the trailing edge (Fig.4) to a value of 2.8 which is beyond the separation criterion. Even though both methods are using the same boundary layer code, the results are different. The reason for this is the different approach used in the calculation methods. In the design process starting with the inverse velocity distribution, the boundary layer displacement thickness is subtracted from the potential profile. The resulting profile, called the "metal profile", is used as input into the direct calculation. Due to the reduced rear thickness, the diffusion of this profile is higher resulting in thicker boundary layers and higher shape factors. In the present case the direct calculation therefore predicts suction surface separation near the trailing edge.

After finishing the design process it was not clear whether or not the profile was free from separation at the design point. For this reason, an experimental verification was carried out which also provided the actual operating range of the cascade.

III. FACILITY AND MEASUREMENT TECHNIQUE

The cascade windtunnel is a continuously running facility operating in a closed loop driven by two radial flow compressors with a flow capacity of $10m^3/s$ each. One of these compressors is connected to the suction system which is used to reduce the upstream side wall boundary layer through protruding slots, to adjust the periodicity by controlling the outer passage pressure recovery, and to vary the axial-velocity-density-ratio through slotted side walls.

The pressure ratio of four renders a possible Mach number range from 0.2 to 1.4 and a variation of the axial-velocity-density-ratio even at supersonic inlet velocities. The cascade span is 168mm and the cascade height can be varied between 150mm and 450mm. Fig.5 shows a cross section of the tunnel. The blades are mounted between Plexiglas windows in the rotatable side walls of 2m diameter. The upper floor is fixed and carries a variable half nozzle and at the rear a slotted transonic floor connected to the suction system which was closed in the present tests. The bottom floor can be moved horizontally and vertically to adjust the geometry of the bottom by-pass passage.

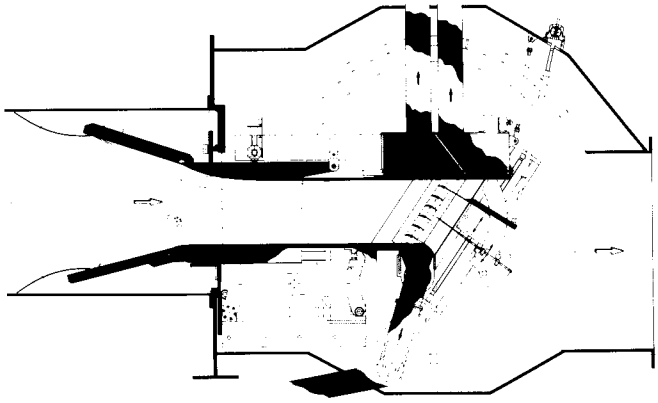

Fig.5: Cross sectional view of transonic cascade wind tunnel

A probe traversing system is mounted in the downstream tunnel area and provides a rotation of the probes around the upstream probe head. The traversing is generally carried out at cascade midspan.

For the test series seven blades of 70mm chord length were installed in the windtunnel. The fourth blade was equipped with 10 pressure taps on the suction side and the fifth with 10 pressure taps on the pressure side in such a way, that the flow in one blade passage could be recorded. The local surface Mach number was calculated using the upstream total pressure. In order to vary

the axial-velocity-density-ratio, side wall slots were provided in the cascade passage as shown in Fig.6.

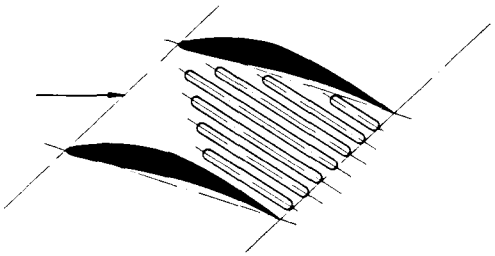

Fig.6: Side wall suction slots

Inlet total pressure and temperature were measured in the settling chamber. In a plane half a gap axially upstream of the leading edges, the inlet static pressure was measured ahead of the center blades at one side wall. In the same plane the inlet flow angle was checked by three flow angle probes (Fig.7).

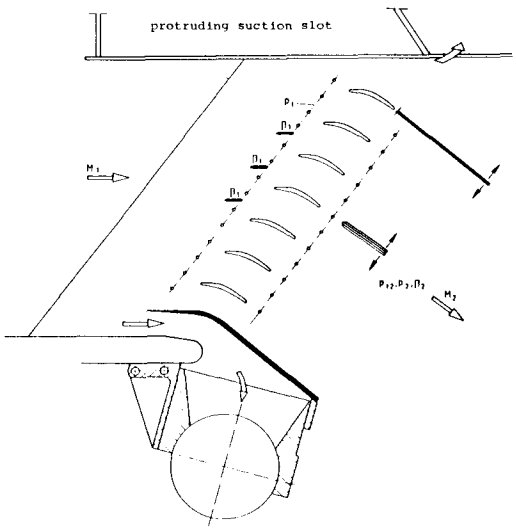

Fig.7: Test section arrangement

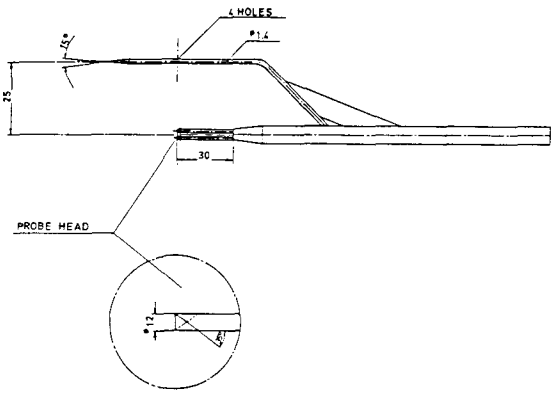

Fig.8: Combined downstream probe

In a plane half a gap axially downstream of the trailing edges the total pressure, static pressure and flow angle distribution were measured by moving a combined probe (Fig.8) stepwise over slightly more than one blade pitch at cascade midspan.

The final data evaluation was carried out off-line on the central computer using the two-dimensional momentum method as described by P. Schimming and H. Starken in Ref. /12/. In this method the downstream measured flow distributions are transferred to uniform conditions by application of the continuity, the energy, and two momentum equations. The final test data, therefore, include a mixing process downstream of the cascade resulting in small corrections of total pressure loss, static pressure rise and exit flow angle. In this calculation no variation of the axial velocity density ratio between the measuring and the far downstream plane is considered.

IV. TEST RESULTS

The test series were performed by varying the inlet Mach number at fixed inlet flow angles, keeping the AVDR as close as possible to the design value of Ω=1.10. Some of the resulting loss curves are shown in Fig.9 and Fig.10. Fig.9 presents the curves at positive and Fig.10 the corresponding curves at design and negative incidences.

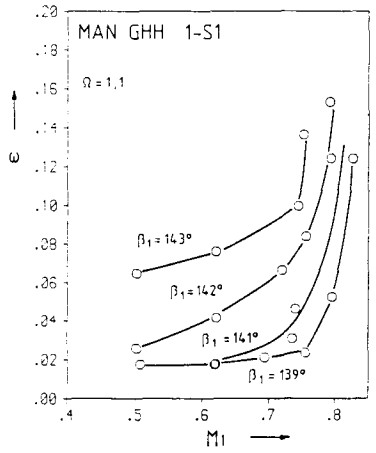

Fig.9: Loss development with Mach number at positive incidences

These curves show the typical loss behaviour with inlet Mach number of a compressor cascade. At positive incidences this is characterized by an overall loss rise at higher inlet flow angles whereby the final steep loss rise is only slightly affected by β_1. Contrary to this, at negative incidences the final loss rise moves to lower inlet Mach numbers with decreasing inlet flow angle due to choking of the cascade. The highest Mach number range is achieved at β_1=139° or two degrees of incidence.

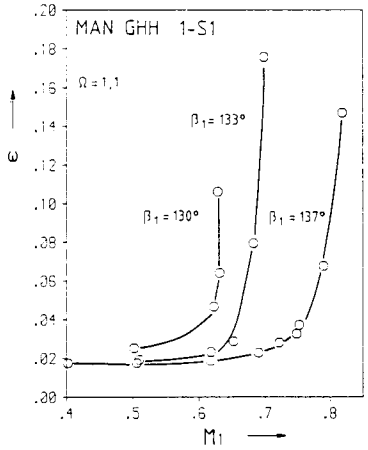

Fig.10: Loss development at design and negative incidences

More interesting, however, than these curves are the loss data plotted as function of the inlet flow angle as presented in Fig.11 with the inlet Mach number as independent parameter and for the design AVDR of Ω =1.1. The resulting curves show a large operating range of the cascade at the design inlet Mach number of M_1=0.62. If a four percent loss level is taken as limiting value, the range extends from i=+5.0° to i=-6.5°. With increasing inlet Mach number, this operating range is, of course, considerably reduced mainly due to choking of the cascade, and the range is thereby shifted to higher incidences with a minimum loss level at β_1=139°. The corresponding dependencies of the exit flow angle and the static pressure ratio of the cascade are shown in Fig.12 and Fig.13. Taking into account the measurement accuracy of the exit flow angle with $\pm$0.3° the agreement with the design values is excellent. For a complete valuation of these data also the axial-velocity-density-ratio (AVDR) influence has to be considered. The corresponding dependencies are shown in Figs.14-16 for the design inlet flow condition. In the measured range no influence on the losses but, of course, on the exit flow angle and on the pressure ratio was observed. However, in the loss rise regions the losses depend also on Ω.

The favourable result of the low loss level at the design point is due to the extended laminar boundary layer on the suction surface combined with a separation free turbulent recompression. A comparison of the measured surface Mach numbers with the inviscid direct calculation (Fig.17) shows very good agreement and confirms the design intent. Flow visualization by releasing ink through surface pressure taps showed a laminar separation bubble around 50 percent of chord and an unseparated turbulent recompression on the suction side.

This favourable behaviour continues at positive incidences up to the point where the transition point on the suction surface moves upstream to the leading edge, which is, of course, related to the position of the maximum velocity point. This condition is reached around β_1=141°. The experimental and theoretical velocity distribution at this point, as presented in Fig.18, are slightly different, but the suction surface distribution is very similar to that one suggested by Walker /13/ as an optimum distribution. Walker proposed a certain low diffusion "unstable laminar" region to generate natural transition followed by a high turbulent diffusion. The present data confirm this idea of an optimum velocity distribution with a maximum on loading at minimum losses. However, the draw back of this distribution is also quite obvious from Fig.11. By an incidence increase of only one degree the loss coefficient rises by a factor of 2.5. Due to the suction peak at this inlet flow angle (Fig.19) the transition point moves to the leading edge causing turbulent separation near 60% of chord. The "Walker distribution" like that one of Fig.18 is therefore only

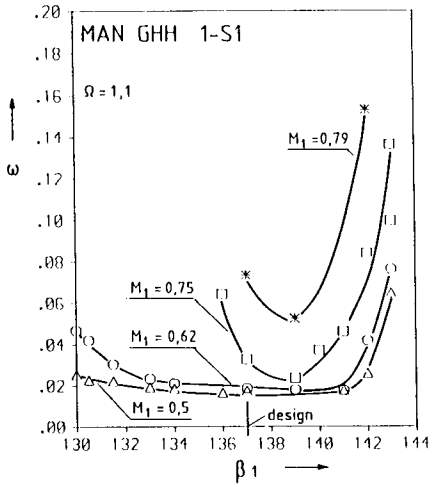

Fig.11: Loss coefficient versus inlet flow angle

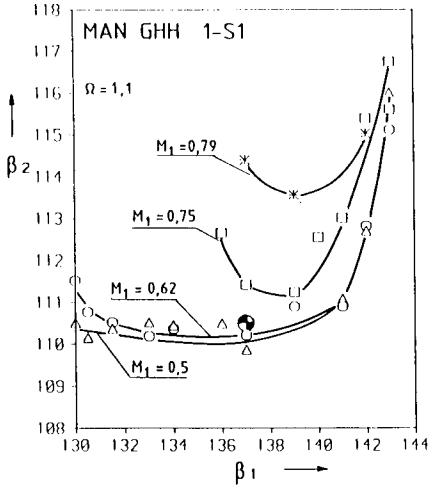

Fig.12: Exit flow angle versus inlet flow angle

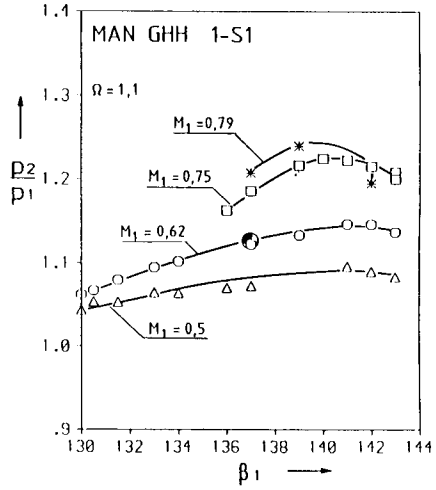

Fig.13: Static pressure ratio versus inlet flow angle

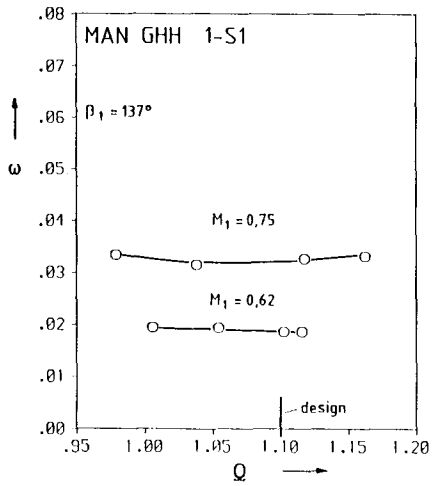

Fig.14: Loss coefficient versus axial velocity density ratio

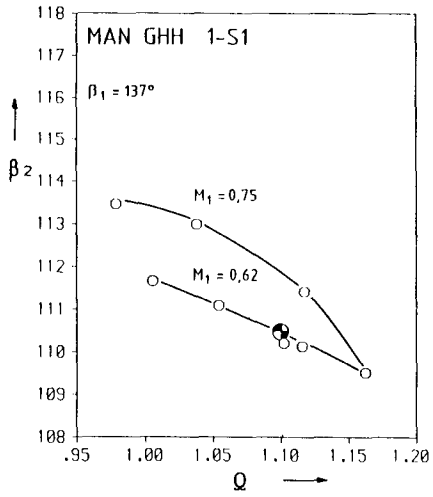

Fig.15: Exit flow angle versus axial velocity density ratio

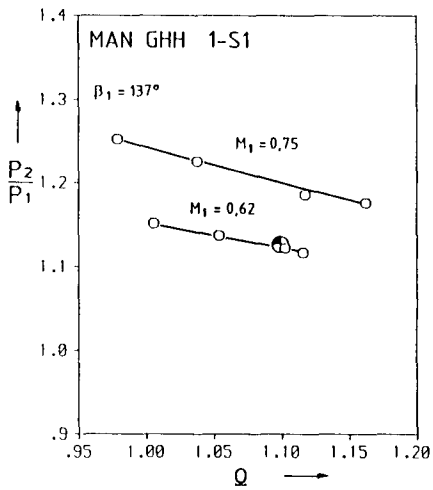

Fig.16 Static pressure ratio versus axial velocity density ratio

useful if a profile is to be designed at maximum incidence condition and not, as usual, at the design operating point of the turbomachine.

With increasing negative incidences the suction surface peak velocity around 45% of chord is rising considerably leading to higher turbulent diffusion, thicker boundary layers and, consequently, higher losses. Around minus four degree of incidence sonic velocity is reached (Fig.20) and at minus seven degree the cascade is very near to choking which was measured at M_1=0.63. In the latter case (Fig.21) shock waves lead to boundary thickening and separation on the suction surface and therefore to a further loss rise. In Fig.22 the measured wake traverses are shown at 0°, -4°, and -7° of incidence and design inlet Mach number. The loss rise is clearly caused by separation on the suction side because the wake is extending to this side. The negative incidence range is therefore limited by suction surface separation just prior to choking of the cascade. This is identical to the loss behaviour of supercritical cascades but different from subsonic ones, which are generally limited by pressure surface leading edge separation. There is a surprisingly good agreement between the measurement and the inviscid prediction in Fig.21 although the suction surface boundary layer is completely separated behind 50% of chord. This confirms the observations in other cascade

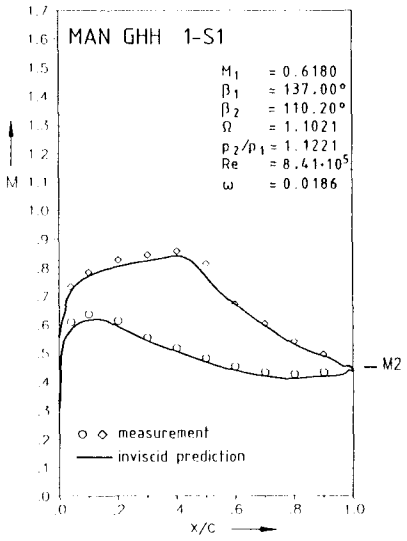

Fig.17: Predicted and measured surface Mach numbers at design condition

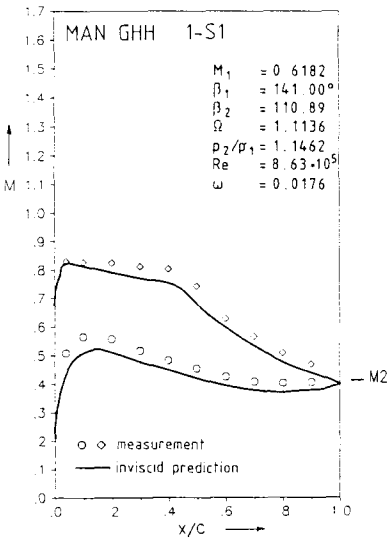

Fig.18: Predicted and measured surface Mach numbers at +4° of incidence

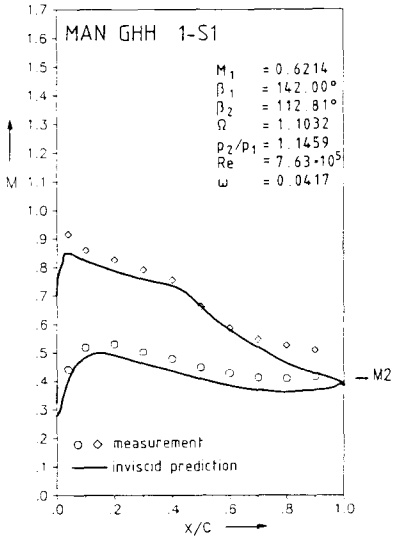

Fig.19: Predicted and measured surface Mach numbers at +5° of incidence

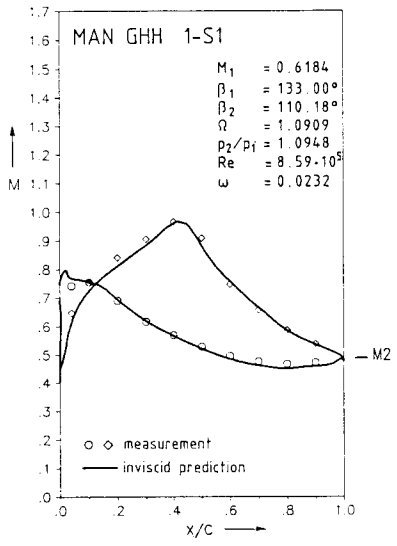

Fig.20: Predicted and measured surface Mach numbers at -4^{o} of incidence

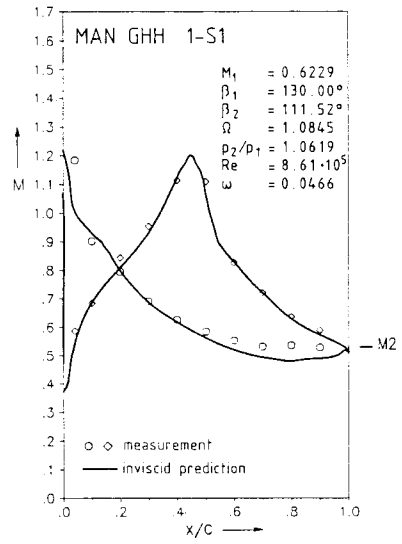

Fig.21: Predicted and measured surface Mach numbers at -7^{o} of incidence

tests, especially high speed ones, that profile separations are not necessarily connected with near constant pressures along the surfaces. The pressure rise within the separated area leads to considerable back flow from the trailing edge to the separation point as has been visualized in other tests. The structure of the flow within the separated area is probably responsible for the different pressure distributions generated along the surfaces.

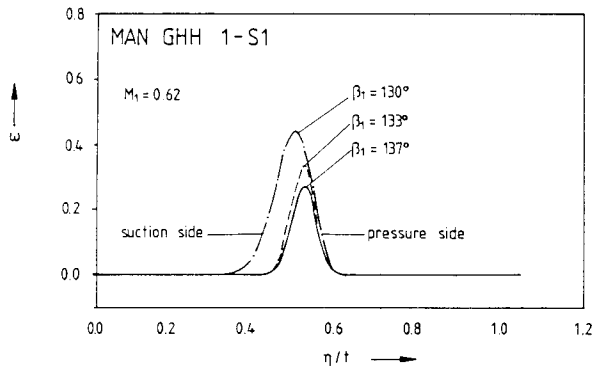

Fig.22: Total pressure loss distribution measured behind the cascade

V. CONCLUSION

By combining a boundary layer calculation with an inverse and a direct flow calculation method a successful optimization of a compressor cascade blade section with regard to low losses and acceptable incidence range was achieved. The velocity distribution developed in this design resulted in a minimum loss coefficient of 1.8%, a positive incidence range of 5^{o}, and a negative incidence range of 6.5^{o} (4% loss level) at an inlet Mach number of 0.62.

The inviscid prediction of the surface Mach number distribution agrees very well with the experimental results at negative incidences even under separated conditions. At positive incidences some differences were observed.

The experiments revealed a separation free operation of the cascade at the design point and confirmed, therefore, the inverse design velocity distribution rather than the prediction which used the metal profile to calculate the boundary layer behaviour and resulted in a rear separation.

VI. ACKNOWLEDGEMENT

The authors wish to thank the MAN GHH for their permission to publish this paper.

VII. REFERENCES

/1/ Turanskyj, L.; Voss, H.
"Recent developments to increase operating efficiences and performance of industrial axial-flow compressors".
IMechE 1987

/2/ Schmidt, E.; Klimetzek, F.
"Verlustarme, superkritische Schaufelgitter".
FVV-Forschungsberichte, Heft 344-1, 1984

/3/ Weber, A.; Rechter, H.; Starken, H.
"Verlustarme, superkritische Verdichterprofile".
FVV-Forschungsberichte, Heft 344-2, 1984

/4/ Schmidt, E.; Klimetzek, F.
"Verlustarme, superkritische Schaufelgitter".
FVV-Forschungsberichte, Heft 392-1, 1987

/5/ Weber, A.; et al.
"Verlustarme, superkritische Schaufelgitter".
FVV-Forschungsberichte, Heft 392-2, 1987

/6/ Schmidt, E.
"Numerische Berechnung und experimentelle Untersuchung des transsonischen Strömungsfeldes in stark umlenkenden Schaufelgittern".
Dissertation Universität Stuttgart (1976)

/7/ Schmidt, E.
"Computation of Supercritical Compressor and Turbine Cascades with a Design Method for Transonic Flows".
Trans. ASME, J. Eng. Power, Vol. 102, Jan. 1980, pp. 68-74

/8/ W. D. McNally
"FORTRAN Program for Calculating Compressible and Turbulent Boundary Layers in Arbitrary Pressure Gradients".
NASA TN D-5681, Washington, May 1970

/9/ Schmidt, E.; Grein, H.-D.
"Verdichterbeschaufelungsentwurf".
FVV-Forschungsberichte, Heft 433, 1989

/10/ Lucci, C. W.; Schmidt, W.
"Nachrechnung transsonischer Gitter".
Dornier-Bericht Nr. 79/25B

/11/ Weber, A.; et al.
"Theoretical and Experimental Analysis of a Compressor Cascade at Supercritical Flow Conditions".
ASME-Paper 87-GT-256, 1987

/12/ Schimming, P.; Starken, H.
"Data Reduction of Two-Dimensional Cascade Measurements".
AGARD-AG-207, 1975

/13/ Walker, G. J.
"A Family of Surface Velocity Distributions for Axial Compressor Blading and their Theoretical Performance". ASME-Paper No. 75-GT-34, 1975

VIII. APPENDIX

Suction side		Pressure side	
X	Y	X	Y
0.00417	0.00157	0.00455	-0.00155
0.00490	0.00459	0.00555	-0.00369
0.00572	0.00605	0.00685	-0.00526
0.00787	0.00857	0.01065	-0.00740
0.01938	0.01838	0.01935	-0.00875
0.02919	0.02479	0.02915	-0.00917
0.03929	0.03051	0.03924	-0.00949
0.04910	0.03558	0.04904	-0.00969
0.06161	0.04158	0.06154	-0.00975
0.07421	0.04723	0.07414	-0.00961
0.08672	0.05255	0.08665	-0.00931
0.09913	0.05757	0.09905	-0.00889
0.11163	0.06237	0.11155	-0.00834
0.14295	0.07346	0.14285	-0.00677
0.17426	0.08335	0.17415	-0.00440
0.23678	0.09986	0.23666	0.00140
0.29919	0.11229	0.29907	0.00728
0.36170	0.12045	0.36157	0.01240
0.42431	0.12372	0.42418	0.01691
0.48680	0.12075	0.48668	0.02062
0.54929	0.11249	0.54918	0.02329
0.61168	0.10105	0.61159	0.02444
0.67426	0.08663	0.67419	0.02379
0.73674	0.07003	0.73668	0.02099
0.79922	0.05164	0.79918	0.01607
0.86160	0.03288	0.86157	0.00844
0.92287	0.01438	0.92286	-0.00040
1.00044	-0.00924	1.00022	-0.01424

Table 1: Profile coordinates MAN GHH 1-S1